Available online at www.CivileJournal.org

Civil Engineering Journal

Vol. 2, No. 11, November, 2016

Thermal-Mechanical Coupled Manufacturing Simulation in Heterogeneous Materials

A. El Amri [a *], M. El Yakhloufi Haddou [a], A. Khamlichi [b]

[a] *Department of Physics, Faculty of Sciences at Tetouan, Tetouan 93030, Morocco.*

[b] *Departments TITM, National School of Applied Sciences, Tetouan 93030, Morocco.*

Received 14 May 2016; Accepted 27 November 2016

Abstract

This work is aimed to investigate on thermal and thermo-mechanical behaviour of 6061 Aluminium alloy. The main target of the present investigation is to apply a numerical procedure to assess the thermo-mechanical damage. Finite element analyses of the notched tensile specimens at high temperature have been carried out using ABAQUS Software. The objective was to study the combined effects of thermal and mechanical loads on the strength and ductility of the material. The performance of the proposed model is in general good and it is believed that the presented results and experimental–numerical calibration procedure can be used in practical finite-element simulation.

Keywords: Continuum Damage Models; Manufacturing; Thermal and Mechanical Damage; Finite Element Analysis.

1. Introduction

The Finite element modeling (FEM) has been widely introduced into the design of manufacturing products because of its high efficiency in predicting several problems and major defects occurring in sheet metal forming manufacturing process like necking. In order to predict those defects within a virtual manufacturing system [1-2], One of the most widely used models is continuum damage. The tensile strength, the yield strength and Young's modulus depend the temperature because Young's modulus of some tempered steels increases slightly at mid temperatures before decreasing at high temperature on mechanical properties is linked to transformations of the material structure due to various processes that inelastic deformation can occur more easily at elevated temperatures, so more plastic deformation and creep occur in the plastic zone of a fatigue crack [3, 4]. The damage parameter is not incorporated into the constitutive equation and it is assumed that presence of voids does not significantly alter the behavior of the material. The von Mises criterion is most frequently used as yield criterion in uncoupled models, Damage parameter is incorporated into constitutive equation and crack growth simulation is automatically performed using a complete deterioration of elements in front of the crack tip [5].

To describe the phenomenon of initiation and growth of cavities and micro cracks induced by large deformation in metals and called "ductile damage", within the framework of continuum damage models, either phenomenological or micromechanically based, have been developed. In recent years, several different formulations for a variety of materials and processes have been presented, such as elastic-brittle [6, 7], brittle, creep, fatigue and creep-fatigue [8-13], among others. However, initially, the development and application of damage models was focused on ductile fracture.

Ductile fracture process is controlled by nucleation, growth and coalescence of micro voids, so it is natural to link material fracture behavior to the parameters that describe the evolution of micro voids rather than conventional global fracture parameters [14].

* Corresponding author: abdelouahid26@gmail.com

In this work, the 6061 Aluminum alloy was studied in order to find out the effect of tensile strength. Both the malleability and the ductility properties relate to the plasticity of the material. Malleability refers to the ability of plastic deformation under compressive loads, while ductility refers to plastic deformation under tensile loads.

2. Continuum Damage Mechanics Model for Ductile Materials

Kanchanov defined a continuum damage variable as the relationship between the sectional area of voids A_v and the overall sectional area A_0 of a given surface in a volume element Equation 1. This definition is the same one as the micro-void area fraction used is some micromechanical theories, such as McClintock's [15]. The damage variable can assume any value between 0 and 1, covering from a virgin state to a completely damaged reaches a critical value, when the effective area can no longer resist the applied load, loading to the formation of a macroscopic crack.

$$D = \frac{A_v}{A_0} = 1 - \frac{A_{eff}}{A_0} \tag{1}$$

Where A_{eff} is the effective resisting area. It may observe that.

According to Lemaitre's damage model and strain equivalence principle, any constitutive equation for a damaged material may be derived in the same way as for virgin material, replacing the stress tensor σ by the effective stress tensor $\breve{\sigma}$, defined by:

$$\tilde{\sigma} = \frac{\sigma}{1-D} \tag{2}$$

The effective elastic modulus of damaged material, giving an indirect way to measure the damage in a solid, by monitoring the evolution of the Young modulus with increasing strain:

$$D = 1 - \frac{\tilde{E}}{E} \tag{3}$$

$\breve{E}$ is the effective elastic modulus and E is the elastic modulus for the undamaged material.

The evolution of an internal thermodynamic state variable can be derived assuming the existence of a potential of dissipation ϕ and an associated variable Y, named damage strain energy release rate and defined as [16]:

$$-Y = \frac{\sigma_{eq}^2}{2E(1-D)^2}\left[\frac{2}{3}(1+\nu)+3(1-2\nu)\left(\frac{\sigma_H}{\sigma_{eq}}\right)^2\right] \tag{4}$$

$\sigma_{eq} = \sqrt{\frac{2}{3}}\|\sigma^D\|$ is the von Mises equivalent stress, σ^D is the deviatoric stress tensor, ν is the Poisson's ratio and $\sigma_H = \left(\frac{1}{3}\right) tr(\sigma)$ is the hydrostatic stress. Further, Lemaitre [16] shows that the damage evolution can be written as:

$$\dot{D} = \frac{\partial \phi}{\partial Y}(1-D)\dot{p} \tag{5}$$

With $p = \sqrt{\frac{2}{3}}\|\epsilon^p\|$ defined as the accumulated plastic strain and ϵ^p being the plastic strain tensor. The choice of a proper potential of dissipation that can represent experimental results is the core of any CDM model. In Lemaitre and Chaboche's model, the hypothesis of isotropic damage, existence of a strain threshold for damage initiation and linear evolution of the damage with the accumulation plastic strain leads to the following equation for damage evolution:

$$\dot{D} = \begin{cases} 0 & for \quad p < p_D \\ \frac{-Y}{S}\dot{p} & for \quad p \geq p_D \end{cases} \tag{6}$$

p_D: The accumulated plastic strain threshold and
S: The damage resistance parameter, which are material dependent properties.

A critical damage value for the uniaxial stress state D_c which can be calculated with the following equation [16]:

$$D_c = \frac{D_{lc}}{R_v}\left[\frac{\sigma_u}{\sigma_{eq}}\ 1-D\ ^2\right] \tag{7}$$

Where D_{lc} is the critical damage for the uniaxial stress state and can be measured in a tensile test, σ_u is the ultimate stress and R_v is Triaxiality factor, which accounts for the difference between the actual stress state and the perfectly uniaxial stress state.

$$R_v = \left[\ \frac{2}{3}\ \ 1+\nu\ +3\ 1-2\nu\ \left(\sigma_H \big/ \sigma_{eq}\right)^2\right] \tag{8}$$

This model was later implemented in the ABAQUS/Explicit solver using subroutine [17] following the numerical algorithm proposed by lee and Pour-Boughrat [18].

3. Materials and Simulation Method Description

The material considered in this study is 6061 Aluminium Alloy. The main mechanical and thermal properties of tested specimen are summarized in Table 1. The geometry of the tested studied is shown in Figure 1. To obtain a thermal stress loading under homogeneous uniform temperature distribution, the steel was restrained against axial expansion by creating an interaction boundary condition at its outside edge. In order to determine thermal strain in the analysis we have need to the thermal expansion coefficient. Poisson's coefficient does not depend on temperature and takes the constant value.

A displacement boundary condition was applied at the outside extremity of the tensile specimen. The displacement was smoothly ramped up in the first portion of the test and then held constant.

The explicit finite element calculation software, ABAQUS/Explicit, was employed for the simulation of traction deformation and fracture of the 6061 Aluminium alloy. The size of mesh in the element model was 0.05 mm×0.05 mm and 0.1 mm×0.1 mm for the 20 mm and 110 mm sample, respectively. Thus, there were 18785 and 56360 meshes in the 20 mm and 110 mm model, respectively. The mesh was then transitioned toward the boundaries using triangular elements and quad elements where bilinear mapping could be employed. The finite element analysis results are critical for identifying crack propagation parameters during a TMF cycle. The methodology is sensitive to the finite element modelling procedure. Care must be taken in controlling the element selection, material properties definition and applied boundary condition evaluation. The selected element type was an 8-node linear brick, of reduced-integration elements (C3D8R). In the finite element model, the specimen was simplified as a rigid body. The displacement load was applied on the top specimen along the 3-axis direction with the other degrees of freedom fixed. In the traction test, the Steel cylindrical rod suffered damage. The boundary element method (BEM) simplifies the meshing process and has the ability to correctly characterize the singular stress fields near the crack front. The boundary conditions applied to this model were the result of a global/local approach where displacements and temperatures were taken from the results of the global model and applied to the boundaries of the local sub-model studied here. Therefore, in order to gain a further insight into the evolutionary process of the damage to the 6061 Aluminium alloy, a shear damage model built in the standard model library of ABAQUS software was used. The thermal portion of the analysis should consist at least of two steps. The first step is a steady-state analysis in which the blade is brought from an initial temperature of 100 °F to a steady operating temperature distribution and then the second step simulates the cool down. The transient response of the blade is then monitored for flight time.

Table1. Mechanical and Thermal material properties

Density	2700 kg/m^3
Young's modulus	71000 N/mm^2
Poisson's ratio	0.33
Heat capacity [19]	900 J/KgK
Heat conduction [19]	120 W/mk
Thermal expansion coefficient	2.4.10-5 $K-1$

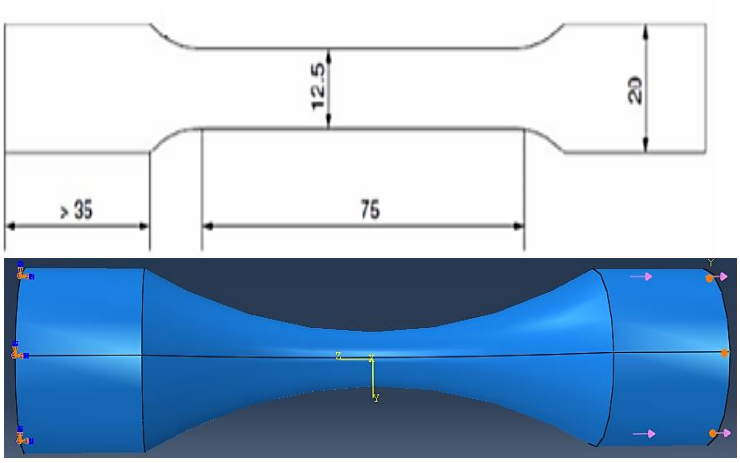

Figure 1. Geometry of the simulated tensile test specimen and boundary conditions (dimension in mm) [20]

4. Results and Discussion

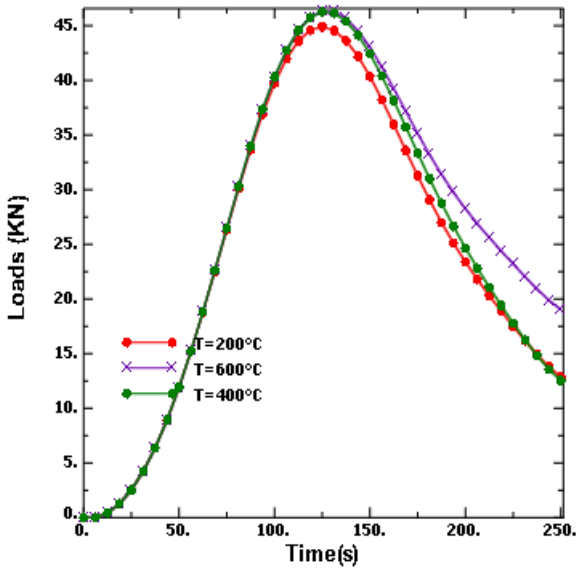

Figure 2. Resulting load- time curves for three different value temperatures

The analysis of the results presented in Figure 2. show that in the first 125 seconds the force Reaches 45.5 KN. The tensile behaviour of the specimens was determined as the load–time relation during tensile loading. Furthermore, a change in the loading curve during time was obtained. Load start, i.e. elastic strain start, then plastic strain start point where the maximum force is reached, i.e. the end of homogenous plastic strain (fracture). The results presented in Figure 2. prove that the maximum elongation before final failure line started. The beginning of elastic deformation, the beginning of plastic deformation, reaching maximum force, the homogeneous plastic deformation to the final fracture of specimen and then the temperature distribution is consistent with the equivalent plastic strain one, which shows that the temperature change causes by the plastic work.

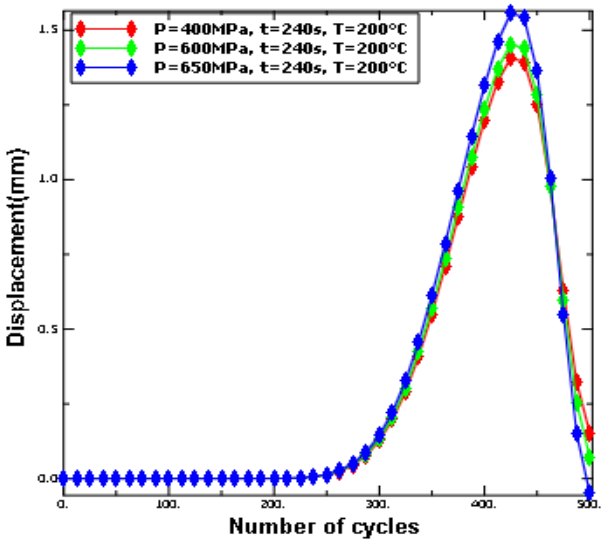

Figure 3. Resulting displacement-Number of cycles curves for three different values Pressure

The Figure 3. depicts the elongation (displacement) measured between the 1st and Nth cycles as a function of the number of cycles. In order to evaluate the influence of the maximum cyclic stress on the dimensional changes of the material, the plastic elongation measured between the 1st and 500th has been plotted as a function of the plastic elongation during the 1st cycle. The plastic elongation between the 1st and 500th cycle increases rapidly with the deformation. Thus the elongation between the 1st and the 500th test cycle initially increase with the maximum stress, then decrease and becomes very small at high stresses. However, the thermo-mechanically coupled problem is not a bifurcation problem, since inelastic heat generation gives rise to an increased temperature in the specimen and convection results in the non-homogeneous temperature distribution. The response is more brittle for the case of combined softening, which is characteristic for metals when loaded in tension.

To demonstrate the influence of the Pressure loads in the model, simulations have been performed with tree different values: 400, 600 and 650 MPa.

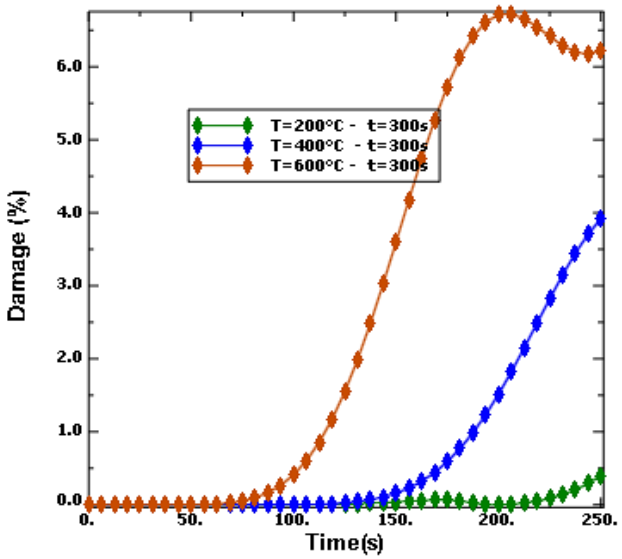

Figure 4. Resulting Damage- time curves for three different values of temperatures

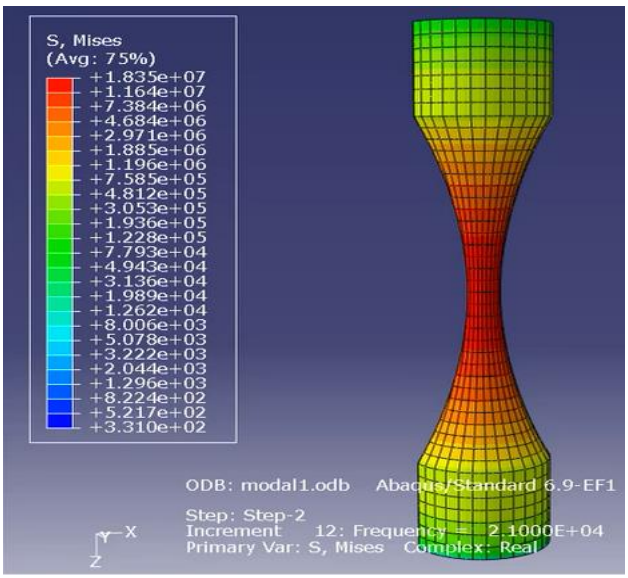

Figure 5. Stress evolution image of the specimen during loading test

During the rapid-growth period exhibited in Figure 5. smaller clusters can continue to grow but they are not necessary to complete the failure. For increasing system sizes the NT onset of rapid growth occurs at earlier times, and so there is less other damage and interactions of the largest cluster with the smaller clusters can be neglected for large system sizes. In the time-dependent problem studied here the heterogeneity is self-generated by the evolution of the damage itself, and there is no heterogeneity in the local failure rates. Furthermore, failure in the present problem is not instantaneous but rather stems from the onset of an accelerating growth process. This latter aspect makes the present problem somewhat more tractable than the time-independent problems, where there is an actual fracture threshold. The damage rate is slightly smaller than the rate of effective plastic strain, as the time, displacement and temperature increases the stress state at the center of the specimen Figure 5. causes the damage to increase exponentially whereas the equivalent plastic strain rate remains approximately constant. The reaction forces on the constrained edge of the specimen it is possible to observe the damage influence on the global behaviour of the structure because the softening caused by damage results on the decrease of the reaction force.

5. Conclusion

This paper has presented a comprehensive numerical study aimed at developing and validating a predictive model of fracture damage in specimen structure under plastic conditions. The material models successfully describe continuum damage mechanics for ductile materials of specimens that are often presented in literature. The method of scaling fracture locus for different temperatures is successful and for plastic response depends on the type of material. The obtained results confirm that it is very useful to use Continuum damage model based on ABAQUS software for early diagnostics of complex metal structures in the exploitation or service conditions. The obtained results prove that the model offers the possibility of non-destructive and real time testing to observe the physical process of metal degradation and to detect the occurrence of energy dissipation. A large-scale grounding experiment is also simulated showing very good agreement with measurements.

6. References

[1]. Bauvineau, L., H. Burlet, C. Eripret, and André Pineau. "Modelling ductile stable crack growth in a C-Mn steel with local approaches." Le Journal de Physique IV 6, no. C6 (1996): C6-33.

[2] Junis, Bašir, Marko Rakin, Bojan Međo, and Aleksandar Sedmak. "Numerical simulation for studying constraint effect on ductile fracture initiation using complete Gurson model." FME Transactions 38, no. 4 (2010): 197-202.

[3] Cabrera, F. Mata, J. Tejero Manzanares, I. Hanafi, A. B. Arenas, I. Garrido, V. Toledano, and M. L. Rubio. "Investigating the deformation and damage scenario under tensile loading of ductile specimens using thermography." International Review of Applied Sciences and Engineering 5, no. 1 (2014): 1-8.

[4] Smerd, Rafal. "Constitutive behavior of aluminum alloy sheet at high strain rates." (2005).

[5] Bergström, J., G. Fredriksson, M. Johansson, O. Kotik, and F. Thuvander, eds. The use of tool steels: experience and research: proceedings of the 6th international tooling conference, Karlstad University, Sweden, 10-13 september 2002. Karlstad University, 2002.

[6] Murakami, S. "Mechanical modeling of material damage." Journal of Applied Mechanics 55, no. 2 (1988): 280-286.

[7] Murakami, Su, and K. Kamiya. "Constitutive and damage evolution equations of elastic-brittle materials based on irreversible thermodynamics." International Journal of Mechanical Sciences 39, no. 4 (1997): 473-486.

[8] Krajcinovic, D., and G. U. Fonseka. "The continuous damage theory of brittle materials, part 1: general theory." Journal of applied Mechanics 48, no. 4 (1981): 809-815.

[9] Krajcinovic, D. "Constitutive equations for damaging materials." Journal of applied Mechanics 50, no. 2 (1983): 355-360.

[10] Simo, J. C., and J. W. Ju. "Strain-and stress-based continuum damage models—I. Formulation." International journal of solids and structures 23, no. 7 (1987): 821-840.

[11] Simo, J. C., and J. W. Ju. "Strain-and stress-based continuum damage models—I. Formulation." International journal of solids and structures 23, no. 7 (1987): 841-869.

[12] Chaboche, Jean-Louis. "Continuum damage mechanics: Part I— General concepts. Journal of applied mechanics 55, no. 1 (1988): 59-64.

[13] Chaboche, Jean-Louis. "Continuum damage mechanics: Part II—Damage growth, crack initiation, and crack growth." Journal of applied mechanics 55, no. 1 (1988): 65-72.

[14] Abendroth, Martin, and Meinhard Kuna. "Determination of deformation and failure properties of ductile materials by means of the small punch test and neural networks." Computational Materials Science 28, no. 3 (2003): 633-644.

[15] McClintock, Frank A. "A criterion for ductile fracture by the growth of holes." Journal of applied mechanics 35, no. 2 (1968): 363-371.

[16] J. Lemaitre, "A Course on Damage Mechanics," 2nd Edition, Springer, Berlin, 1996. doi:10.1007/978-3-642-18255-6

[17] Simulia Abaqus 6.10, "User Subroutines Reference Manual," 2010.

[18] Lee, Sang Wook, and Farhang Pourboghrat. "Finite element simulation of the punchless piercing process with Lemaitre damage model." International journal of mechanical sciences 47, no. 11 (2005): 1756-1768. doi:10.1016/j.ijmecsci.2005.06.009.

[19] A.H. van den Boogaard, "Thermally Enhanced Forming of Aluminium Sheet", Ph.D. Thesis, University of Twente, 2002.

[20] Palumbo, G., and L. Tricarico. "Numerical and experimental investigations on the warm deep drawing process of circular aluminum alloy specimens." Journal of materials processing technology 184, no. 1 (2007): 115-123.